

ASSOCIATIE EURATOM-FOM
FOM-INSTITUUT VOOR PLASMAFYSICA
RIJNHUIZEN — NIEUWEGEIN — NEDERLAND

TANGENTIAL THOMSON SCATTERING

by

C.J. Barth

Rijnhuizen Report 87-173

This work was performed as part of the research programme of the association agreement of Euratom and the 'Stichting voor Fundamenteel Onderzoek der Materie' (FOM) with financial support from the 'Nederlandse Organisatie voor Zuiver-Wetenschappelijk Onderzoek' (ZWO) and Euratom.

CONTENTS

| | Page |
|--------------------------------------------------------------------------------|------|
| 1. Introduction | 02 |
| 2. The TORTUR experiment | 06 |
| 3. The polychromator for v_d -measurements | 08 |
| 4. The polychromator for recording non-thermal electron velocity distributions | 08 |
| 5. Experimental set-up | 10 |
| 6. The detection limit for observation of v_d and of the tail distribution | 13 |
| 6.1 Expected error for the observation of v_d | 13 |
| 6.2 The detection limit for observation of the tail distribution | 14 |
| 7. Conclusion | 16 |
| Acknowledgement | 17 |
| References | 17 |

1. INTRODUCTION

Thomson scattering [1] is one of the most useful diagnostics to determine the local electron temperature and density of thermonuclear plasmas. In the present devices used in fusion research the scattering parameter α [1] is far less than one for 90° scattering with a ruby laser. As a result of this, collective effects can be neglected and only scattering from thermal fluctuations of the electrons are observed.

Normally k_i ($i = \text{incident}$) and k_s ($s = \text{scattered}$) are both in a poloidal plane, which results in an observation of the electron velocity distribution perpendicular to the plasma current direction.

Tangential Thomson scattering, however, with k_s parallel to the direction of the plasma current implies the possibility to detect the drift velocity, v_d [2], and thus the local current density $j = n_e \cdot v_d \cdot e$. Nevertheless, tangential scattering is not applied at present tokamak devices, mainly for two reasons. Firstly, the toroidal field coils drastically limit the access to a tangential viewing port. Secondly, the drift velocity causes only a small shift, $\Delta\lambda_d$, of the observed spectrum as compared to its width, $\Delta\lambda_e$.

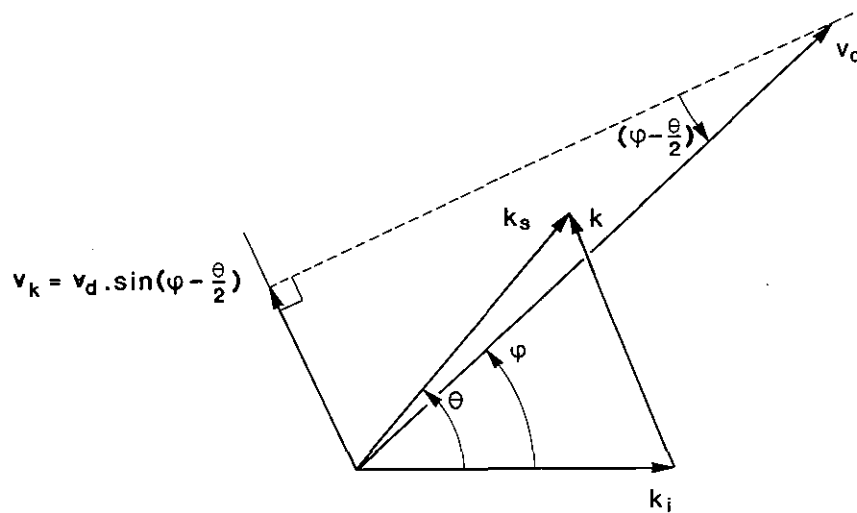


Fig. 1. Geometrical relation between k_i , k_s and v_d .

Referring to Fig. 1, the drift velocity results in a Doppler shift:

$$\frac{\Delta\lambda_d}{\lambda_o} = \frac{2v_k \cdot \sin\theta/2}{c} \quad (1)$$

with

$$v_k = v_d \cdot \sin(\phi - \theta/2) . \quad (2)$$

If the scattering plane is tilted by an angle ξ with respect to v_d , the wavelength shift, $\Delta\lambda_d$, finally will be:

$$\Delta\lambda_d = \frac{2\lambda_o \cdot v_d \cdot \sin\theta/2 \cdot \sin(\phi - \theta/2) \cdot \cos\xi}{c} . \quad (3)$$

In case of 90° scattering with a ruby laser ($\lambda_o = 694.3$ nm) and $v_d \perp k_i$

$$\Delta\lambda_d = \frac{\lambda_o \cdot v_d \cdot \cos\xi}{c} = 2.31 \times 10^{-6} v_d \text{ (nm)} , \quad (4)$$

which should be compared with the thermal width:

$$\Delta\lambda_e = 1.936 \sqrt{T_e} \text{ (nm)} \quad (5)$$

with

$$v_d \text{ in m/s and } T_e \text{ in eV.}$$

For example for the TORTUR III tokamak [3] at a plasma current of 30 kA and $q(o) \approx 2$, the drift velocity $v_d \approx 7 \times 10^5$ m/s, while $T_e = 600$ eV and $n_e = 6 \times 10^{19} \text{ m}^{-3}$, which results in $\Delta\lambda_d \approx 1.6$ nm and $\Delta\lambda_e = 47.4$ nm.

To achieve an acceptable error in the measurement of the drift velocity the wavelength shift, $\Delta\lambda_d$, should be measured with an accuracy of ± 0.2 nm, which is less than 0.5% of $\Delta\lambda_e$. The usual Thomson-scattering systems have typical observation errors which are about a factor of 10 to 20 higher at comparable plasma properties.

Since 1983 the detection of the Thomson-scattering spectra at TORTUR III was performed with a high (50%) transmission twenty-channel polychromator, covering a wavelength range from 600 to 800 nm and equipped with infrared sensitive photomultipliers (GaAs photocathode, quantum efficiency $\approx 15\%$; Ref. 4). The main purpose of this high sensitivity was to observe small deviations in the scattered spectrum (Fig. 2). With

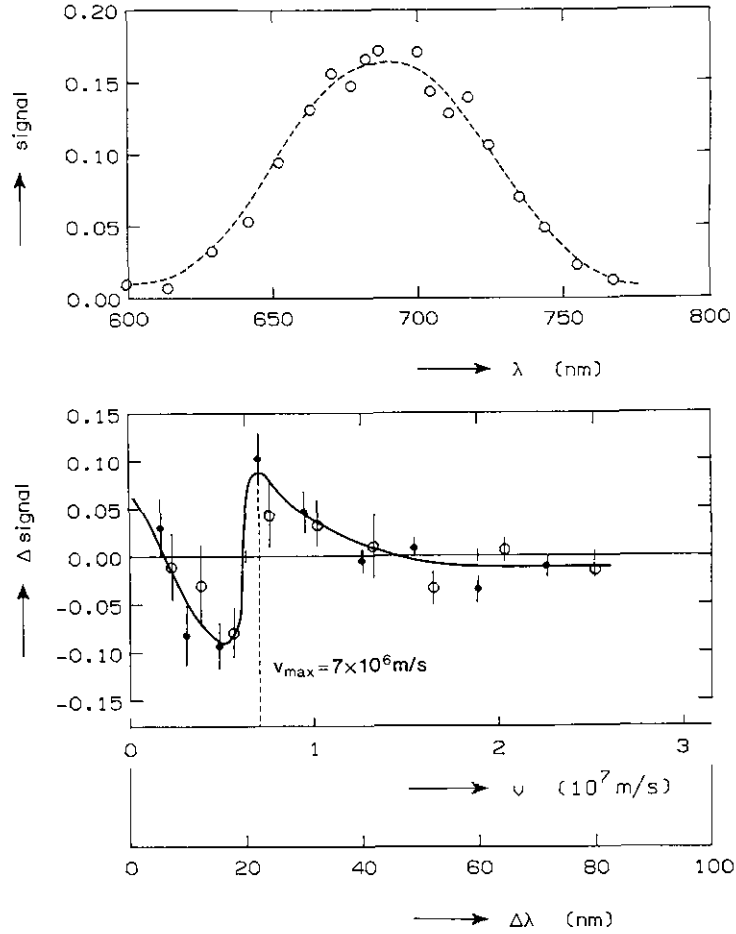


Fig. 2. a) Thomson-scattering spectrum (90° , $\lambda = 694.3$ nm) $T_e = 594 \pm 8$ eV and $n_e = (5.57 \pm 0.07) \times 10^{19} \text{ m}^{-3}$; the dashed line is a relativistic Gaussian fitted to the data. b) Deviations of the data from the Gaussian. The open circles correspond to the red and the filled circles to the blue wing of the spectrum.

this diagnostic tool it is possible to record a wavelength shift with an accuracy of 0.3 nm at $n_e \approx 5 \times 10^{19} \text{ m}^{-3}$ and $T_e \approx 800$ eV.

Besides the measurement of v_d , tangential Thomson scattering offers the ability to observe the tail distribution of the electron population. Incidentally, a tail distribution of several keV has already been observed in radial scattering experiments at the plasma edge ($r = 60$ mm) of the TORTUR III tokamak ($a = 85$ mm, Fig. 3) during a fast current pulse ($\Delta I_p = 30$ kA and $\Delta t = 10 \mu\text{s}$). The observation of the tangential tail distribution is of importance for the interpretation of different plasma phenomena, such as:

- non-thermal ECE spectra [10]
- non-maxwellian velocity distributions found with radial Thomson scattering [7, 8] (see also Fig. 2),
- the amplitude modulation of density fluctuations: 1-500 kHz and magnetic fluctuations: $0.7 < f < 3$ MHz as recorded with collective scattering of microwaves [9, 14, 16].

These phenomena have been studied extensively in the TORTUR III tokamak [14], especially the relation between the fundamental mode of the magnetic fluctuations and the occurrence of satellites on the Thomson-scattering spectra (Fig. 2 shows an example) [9]. For all of the above reasons, we decided to equip the new (TORTUR IV) liner with a tangential viewing port.

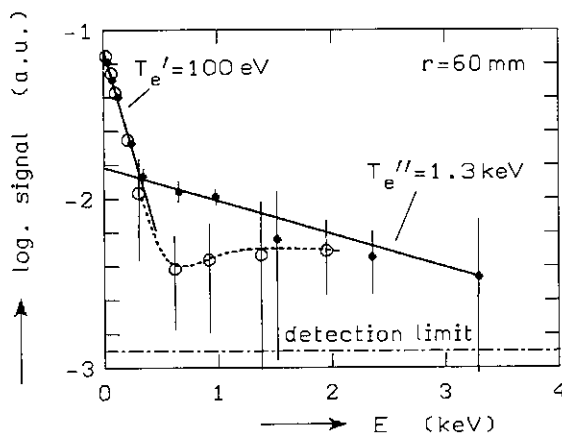


Fig. 3. Observation of a tail distribution at the plasma edge $T_e'' \approx 1.3$ keV (temperature in the poloidal plane) and $n_e'' \approx 2 \times 10^{18} \text{ m}^{-3}$ during a fast current pulse ($\Delta I \approx 30$ kA, $\Delta t_{\text{pulse}} = 10 \mu\text{s}$), while the bulk temperature $T_e' = 100$ eV and $n_e' \approx 2.5 \times 10^{19} \text{ m}^{-3}$. The dots represent the blue, and the open circles the red wing of the spectrum.

This report describes the experimental set-up for tangential Thomson scattering on TORTUR IV:

- the TORTUR experiment,
- the polychromator for v_d -measurements,
- the optical system for tangential scattering,
- the polychromator for recording non-thermal electron distributions,
- the expected accuracy in the determination of the drift velocity and the temperature and density of the tail distribution.

2. THE TORTUR EXPERIMENT

The tokamak TORTUR was originally built to study current-driven turbulence as a possible method for plasma heating [3, 5]. The plasma is confined by means of a toroidal field $B \approx 3$ T within an Inconel liner ($R = 0.46$ m, $a = 0.085$ m) surrounded by a copper shell. After plasma formation the energy of a 1 F capacitor is coupled to the plasma by means of a transformer yoke (0.2 Vs), thus maintaining a current of 30 to 60 kA during 40 to 20 ms, respectively.

Various diagnostics are used to measure the plasma parameters:

- current and loop voltage pick-up coils,
- a soft X-ray pinhole camera [15],
- a hard X-ray detector,
- a neutral particle analyser with an ion beam probe [11],
- spectroscopic measurements in the VUV and visible range,
- a 6-channel ECE spectrometer for the determination of T_e -profiles from $2 \omega_{ce}$ -emission [12],
- a collective Thomson-scattering set-up with a $\lambda_0 = 4$ mm (TORTUR III) and $\lambda_0 = 2$ mm (TORTUR IV) beam probe to study coherent density fluctuations,
- radial Thomson scattering over 90° on thermal fluctuations with a ruby laser system (see Section 3).

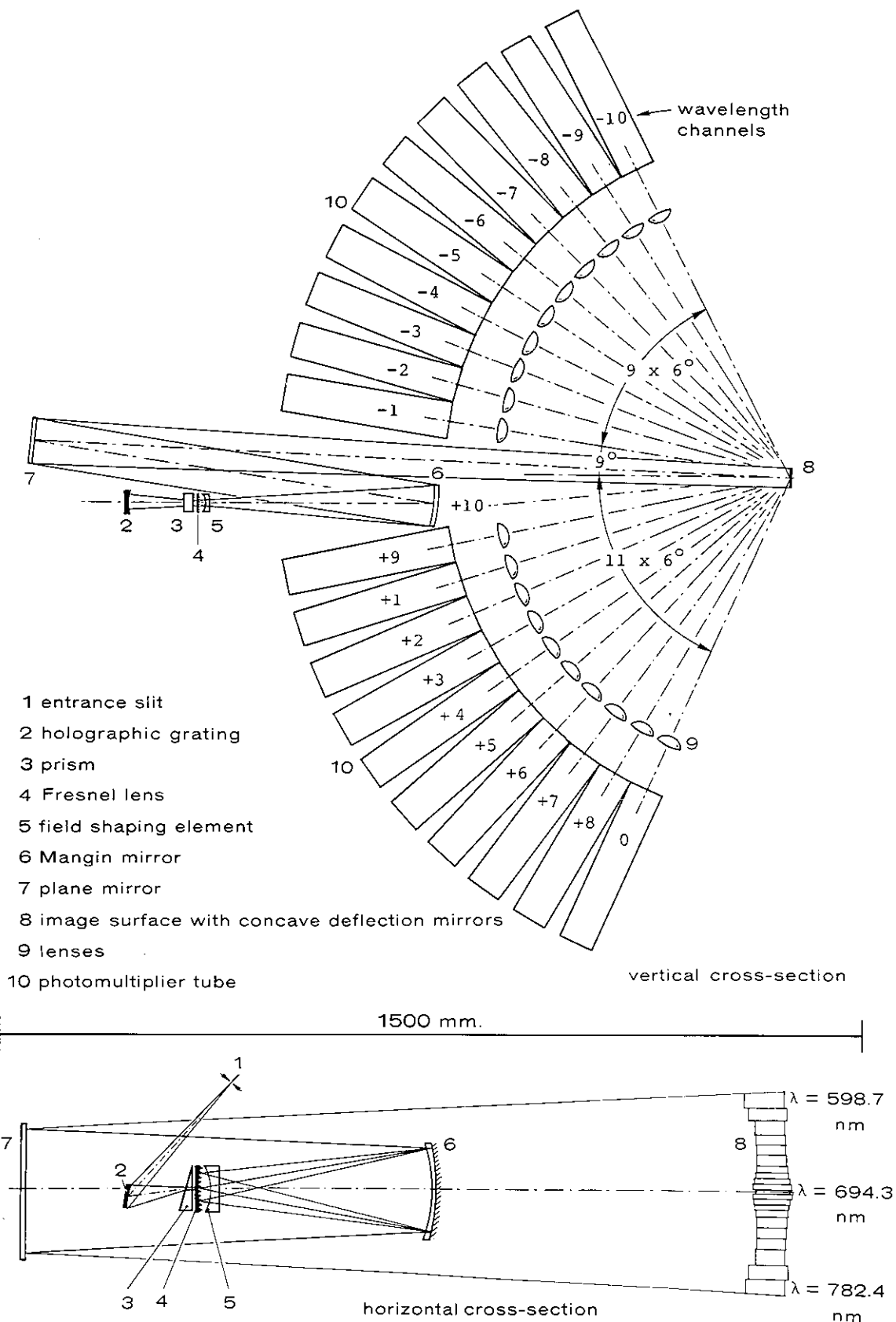


Fig. 4. Vertical and horizontal cross-section of the optical system of the twenty-channel polychromator. After dispersion by the grating (2) the intermediate image of the spectrum is formed between (3) and (4). This image is five times magnified by means of a Mangin mirror (6). Twenty concave mirrors (8) each deflect a small spectral range into the corresponding photomultiplier (10).

3. THE POLYCHROMATOR FOR v_d -MEASUREMENTS

The scattered light is spectrally resolved with a holographically ruled concave grating (Fig. 4). To adapt the spectral image of the grating to the size of the recording photomultipliers, a five times magnification is performed by means of a Mangin mirror. A set of 20 concave wavelength selection mirrors guide the light of the different spectral intervals to the detectors. In this way, the use of fibre optics could be avoided and a transmission of 50% could be obtained. Together with the application of infrared sensitive photomultipliers (with GaAs cathode), a very sensitive diagnostic tool was developed.

The diagnostic properties, as deduced from radial scattering which are of importance for the tangential scattering and its relevant physics are summarized below.

- a. T_e - and n_e -measurements are possible with a 1% error at $n_e \approx 5 \times 10^{19} \text{ m}^{-3}$ and at a laser energy $E_{\text{laser}} \approx 5 \text{ J}$ for $T_e \approx 800 \text{ eV}$.
- b. Determination of the central wavelength of the relativistic gaussian can be performed with an error of 0.27 nm under the same conditions as quoted in a.
- c. Irregularities in the velocity distribution can be observed with an uncertainty of $8.5 \times 10^{16} \text{ m}^{-3}$.

These irregularities mostly appear as satellites on both the red and the blue wing of the spectrum (Fig. 2) and are thought to be related to magnetic fluctuations (e.g. Alfvén waves) [5].

- d. A tail distribution at the plasma edge of several keV and with a partial density of $2 \times 10^{18} \text{ m}^{-3}$ can be observed incidentally with an error of $\pm 20\%$ (Fig. 3). The latter is mainly due to the anomalous high plasma-light level during the injection of a fast current pulse.

The uncertainty in the wavelength shift (sub. b) was determined from many different observations during the plateau phase (with $I_p = 30 \text{ kA}$). The difference between the central wavelength of the spectrum and λ_0 was found to be on average -0.02 nm, while the standard deviation appeared to be 0.27 nm at $n_e \approx 5 \times 10^{19} \text{ m}^{-3}$, $T_e \approx 700 \text{ eV}$ and $E_{\text{laser}} = 6 \text{ J}$.

4. THE POLYCHROMATOR FOR RECORDING NON-THERMAL ELECTRON VELOCITY DISTRIBUTIONS

Due to the relativistic blue shift [13] (Fig. 5), the Thomson-scattering spectra cover a spectral range for which photomultipliers with a conventional S-20 cathode have maximum sensitivity ($\eta = 15\%$). In order to

survey tail-temperatures up to about 20 keV, a wavelength range down to 300 nm should be analysed (see Fig. 5). However, the spectral range will be

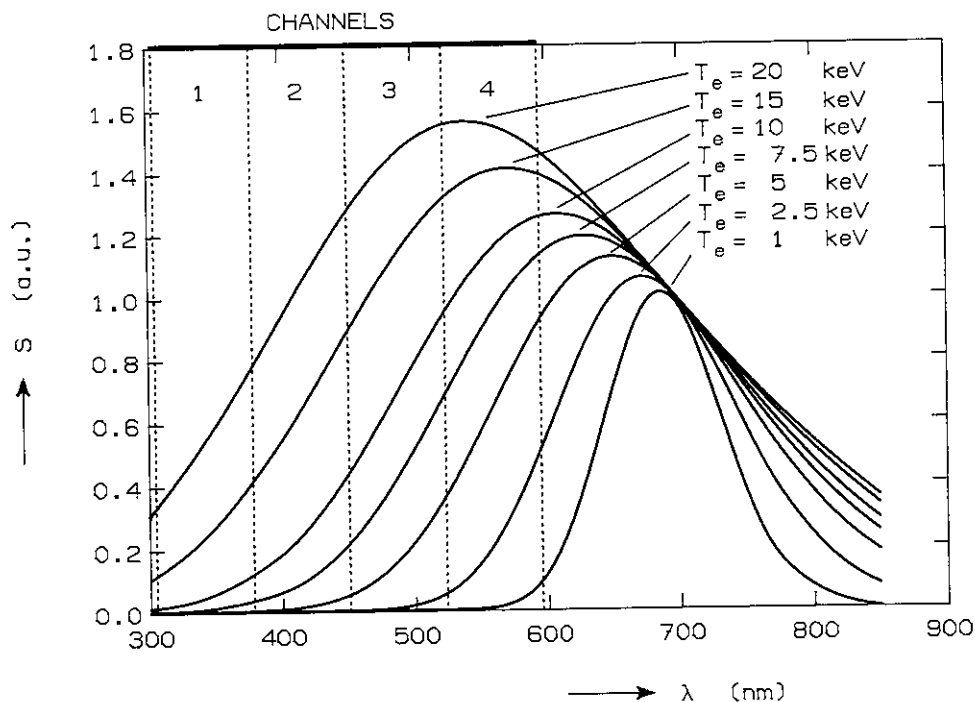


Fig. 5. Relativistic spectra of a thermal tail distribution related to the spectrometer channels.

limited to $\lambda > 350$ nm since the transmission of conventional optical materials used for achromatic lenses, such as BK7 and heavy flint, falls off steeply below 350 nm. To increase the spectral area, one would need achromatic doublets composed of quartz and CaF_2 lenses. Since the price of these achromats is, however, a factor 10 higher than that for conventional ones, we decided to use the latter.

The polychromator constructed is of the Littrow mount. It covers a spectral range from 305 to 595 nm which is divided into four channels (see Fig. 6). Concave spherical mirrors guide the light to EMI 9658 photomultipliers with S-20 cathodes. The polychromator transmission is deduced as follows:

| | |
|--------------------------------|-------------|
| - dichroic filter | 0.85 |
| - input mirror | 0.85 |
| - 2 lenses (coated) | $(0.985)^4$ |
| - grating | 0.80 |
| - wavelength selection mirrors | 0.85. |

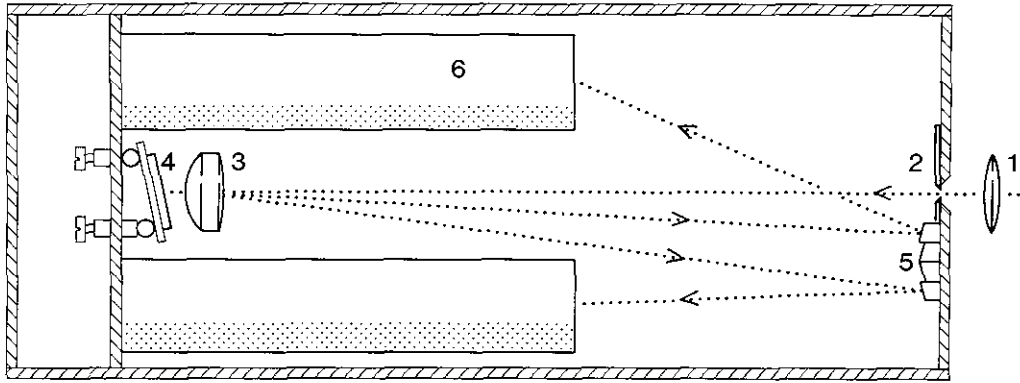


Fig. 6. A 4-channel Littrow-polychromator which covers a spectral area of 305 to 595 nm.

1. field lens
2. entrance slit $2.5 \times 25 \text{ mm}^2$
3. achromatic doublet $f = 500 \text{ mm}$
4. grating 295 l/mm
5. spherical wavelength selection mirrors $R = -331 \text{ mm}$
6. four EMI 9658 photomultipliers.

The transmission of the 4-channel polychromator, being the product of the individual transmissions is about 46%, which is almost similar to that of the twenty-channel polychromator (50%).

5. EXPERIMENTAL SET-UP

The scattering geometry is shown in Fig. 7. The laser beam is directed vertically through the torus and the scattered photons can be collected in two directions:

- a. perpendicular to the toroidal axis for the measurement of $T_{e,\perp}$;
- b. almost parallel to the toroidal axis for the measurement of $T_{e,\parallel}$.

In both situations, the polarization vector (E_ρ) of the laser beam needs to be perpendicular to the scattering plane. Normally, E_ρ is directed parallel to the toroidal axis. In case of tangential scattering, a crystal quartz retardation plate ($\frac{1}{2} \lambda$) is applied to rotate E_ρ over 90° . It is expected that the crystal will not be damaged since its damage threshold of 6.4 GW/cm^2 (measured at $\lambda = 1.06 \mu\text{m}$ and $\Delta t_{\text{pulse}} = 15 \text{ ns}$ [14]) is much higher than the power density of the laser beam (200 MW/cm^2).

The scattered light is led to the twenty-channel polychromator via achromatic lenses and silvered mirrors (Fig. 7). The lens system is chosen such that the solid angle of the diagnostic port is adapted to the polychromator, which results in:

L = height of the scattering volume = 23 mm
 Ω = solid angle = 3.87×10^{-3} sr.

A sapphire prism is used to deflect the scattered beam in such a way that T_e , n_e and v_d can be measured at two alternative vertical positions ($z = 0$ and 46 mm).

A dichroic filter (Fig. 8) is applied to split the scattered light beam into two spectral areas (Fig. 9). In this way, the throughput to the twenty-channel polychromator is only reduced by a factor 0.85 in the wavelength region of interest.

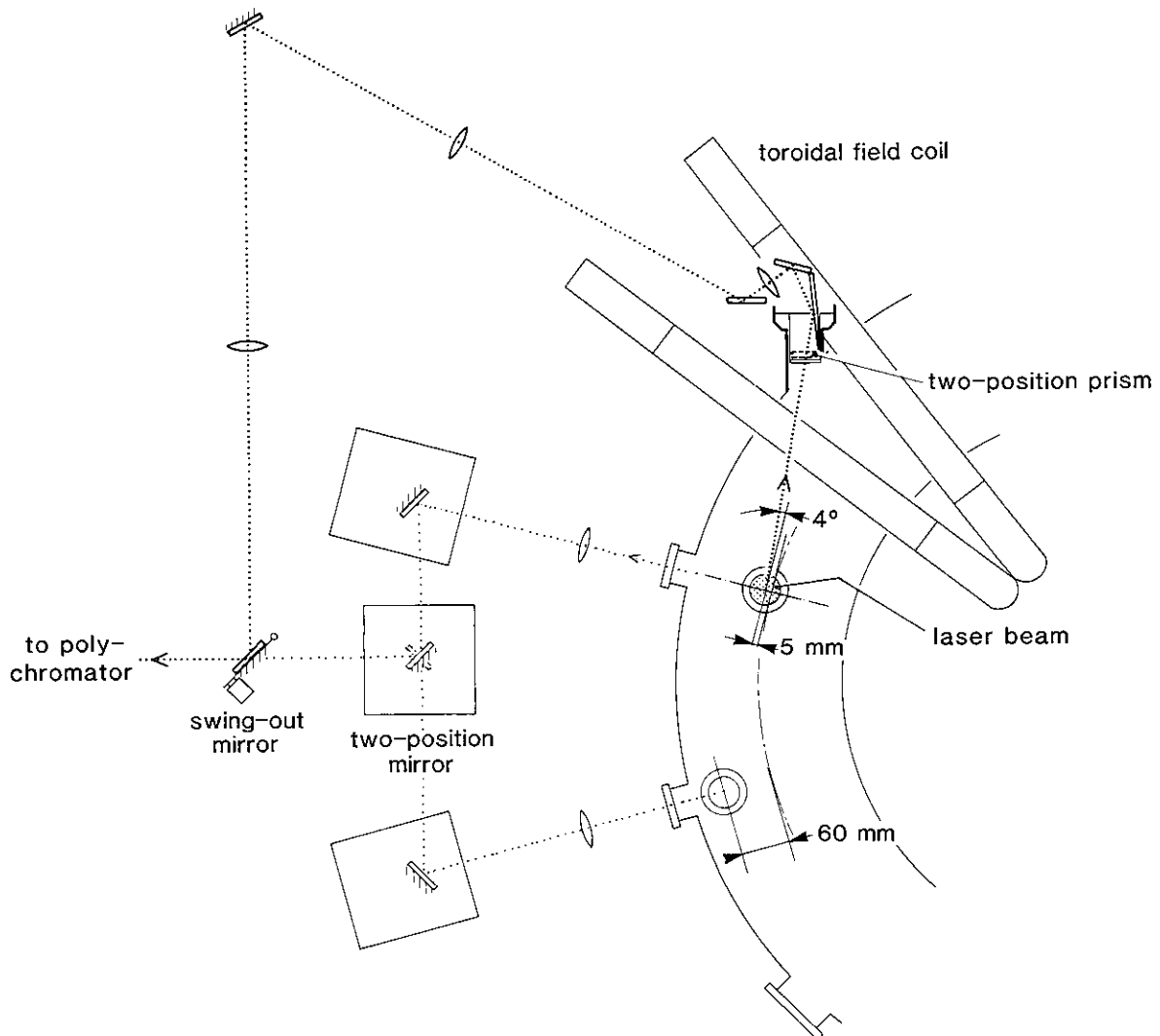


Fig. 7. The geometry for tangential scattering. The laser beam is directed vertically through the plasma. The scattered light can be collected in two alternative directions: parallel and perpendicular to the magnetic axis and is led in either case to the polychromators for recording. Radial scattering can be performed at two alternative positions $r = 5$ mm and $r = 60$ mm.

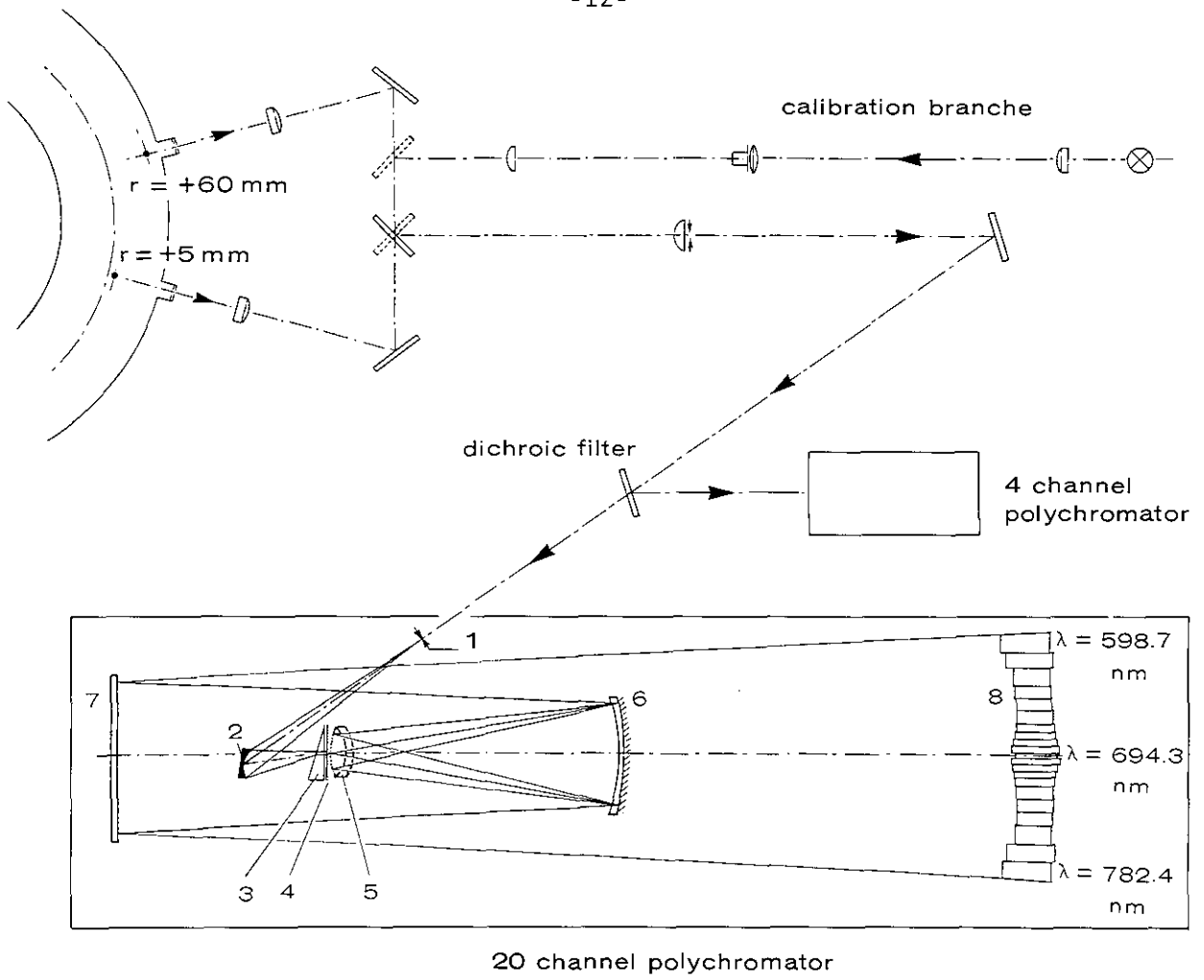


Fig. 8. A dichroic filter is used to split the scattered light into two spectral area's.

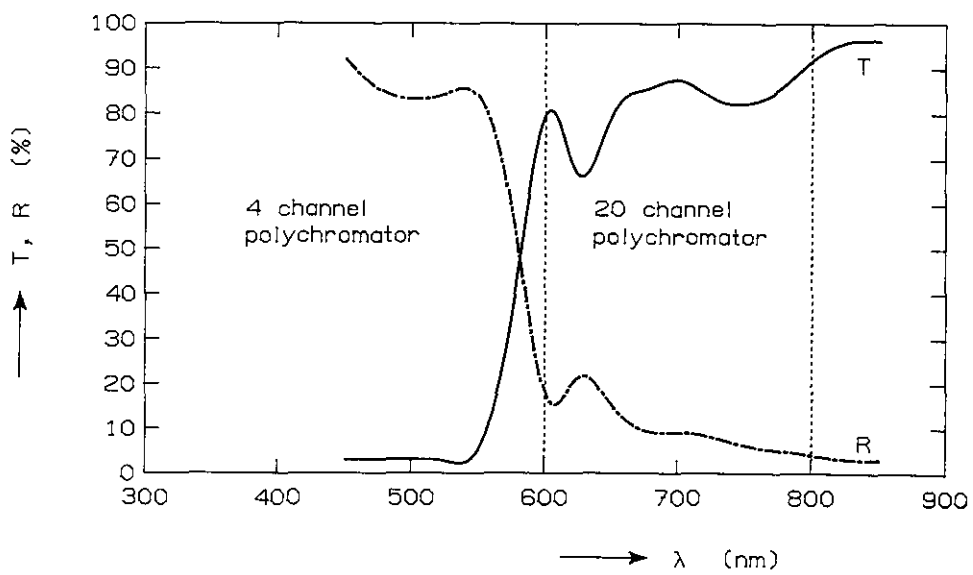


Fig. 9. Spectral response of the dichroic filter
T: transmission
R: reflection.

6. THE DETECTION LIMIT FOR OBSERVATION OF v_d AND OF THE TAIL DISTRIBUTION

6.1 Expected error for the observation of v_d

The detection limit for observation of v_d will be determined mainly by the number of photo-electrons due to Thomson scattering compared to that generated by plasma light emission. For both processes, experimental data have been obtained with the twenty-channel polychromator [4].

The expected number of photo-electrons from Thomson scattering is given by the well-known formula [1]:

$$f_{s,e}(\lambda) = f_i \cdot L \cdot \Omega \cdot \frac{d\sigma_T}{d\Omega} \cdot n_e \cdot T \cdot \eta \cdot S(\lambda) , \quad (6)$$

with:

| | | |
|-----------------------------|-----------------------------------------------------------------------------------------------------------------------------|-----------------------------------------|
| $f_{s,e}$ | number of photo-electrons, | |
| f_i | number of incident photons: | $3.5 \times 10^{18} \times E$, |
| E | laser energy in the scattering volume ≈ 3.5 J; , | |
| | this is $0.6 E_{\text{laser}}$ due to the beam divergence and reflection losses in the focussing lens and the input window, | |
| L | length of scattering volume | 23 mm, |
| Ω | solid angle | 3.87×10^{-3} sr, |
| $\frac{d\sigma_T}{d\Omega}$ | differential Thomson-scattering cross-section, | |
| | (for $\theta = 90^\circ$) | 8×10^{-30} m ² /sr, |
| n_e | electron density | [m ⁻³], |
| T | transmission, product of: | |
| | polychromator transmission (0.50) | } 0.35, |
| | input optics (0.70) | |
| η | quantum efficiency | 0.15, |
| $S(\lambda)$ | fraction of scattered photons collected in the wavelength channel concerned. | |

The observational error in v_d is proportional to the square root of the number of photo-electrons. At a given density and temperature, the number of photo-electrons scales with $\Omega \cdot L \cdot T \cdot \eta$, which is for:

- a. $T_{e,\perp}$ -measurement 9.1×10^{-6} (sr.m) ,
- b. $T_{e,\parallel}$ -measurement 4.4×10^{-6} (sr.m) .

The difference of a factor 2 is mainly due to the smaller solid angle in the tangential scattering set-up (see Fig. 7).

The observational error will mainly be determined by photo-electron statistics since the plasma-light contribution is relatively small as measured in the case of radial scattering ($\leq 1\%$ of the Thomson-scattered light).

The total number(f_e) of photo-electrons recorded can be expressed as a function of the 1/e-width ($\Delta\lambda_e$ in nm) and the height of the gaussian A_1 :

$$f_e = \sqrt{\pi} \Delta\lambda_e A_1 . \quad (7)$$

A small positive shift, $\Delta\lambda_d$, of the gaussian causes an increase of the total recorded number of photo-electrons Δf_e in the channels of the red wing and a corresponding decrease in the blue wing. The relative error for the detection of Δf_e (and thus of $\Delta\lambda_d$) is as follows:

$$\epsilon = \frac{\sqrt{f_e}}{2\Delta f_e} = \frac{\sqrt{f_e}}{2 \cdot A_1 \cdot \Delta\lambda_d} . \quad (8)$$

Together with $\Delta\lambda_e = 1.94 \sqrt{T_e}$ (see Eq. (5)) and Eq. (7) one finds:

$$\epsilon = \frac{1.72}{\Delta\lambda_d} (T_e/f_e)^{1/2} \times 100\% . \quad (9)$$

From the geometrical and instrumental properties mentioned, $f_e = 2.3 \times 10^4$ is expected at $n_e = 5 \times 10^{19} \text{ m}^{-3}$ in the case of tangential scattering. So with a typical value for $\Delta\lambda_d$ of 2 nm and $T_e = 600 \text{ eV}$, one gets $\epsilon = 14\%$ which means that the absolute error in $\Delta\lambda_d$ is 0.28 nm.

However, since f_e is a factor two smaller in the case of tangential as compared to radial scattering one expects from the already available experimental data on radial Thomson scattering (see Section 3) an error of $\sqrt{2} \times 0.27 = 0.38 \text{ nm}$. Under plasma conditions with $q(o) = 1$ and $I_p = 60 \text{ kA}$, one expects for TORTUR IV $v_d(o) \approx 10^6 \text{ m/s}$ and $n_e(o) \approx 10^{20} \text{ m}^{-3}$, which results in $f_e = 4.6 \times 10^4$ and thus:

$$\Delta\lambda_d \approx 1.8 \pm 0.28 \text{ nm} ,$$

when using the error found from experimental data.

6.2 The detection limit for observation of the tail distribution

We have to determine $S(\lambda)$ (see Eq(6)) in order to find the detection limit for the observation of the tail temperature and density. With Fig. 5 in mind it is easy to make a good estimate for $S(\lambda)$ for a tail temperature

of 20 keV. The 1/e-width of the relativistic spectrum is ≈ 220 nm, which means that the total spectrum covers about 600 nm. So each channel of 75 nm collects on average (assuming a triangular shape of the spectrum):

$$S(\lambda) = \frac{75}{600} \times \frac{1}{2} = 0.063 ,$$

and we find:

$$f_{s,e}(\lambda) \approx 2.72 \times 10^{-17} \cdot n_e . \quad (10)$$

Thus at $n_e = 2 \times 10^{18} \text{ m}^{-3}$ about 54 photo-electrons are recorded per channel.

It is difficult to make an estimate of the density limit since the contribution from plasma light in the wavelength area considered (300-600 nm) is unknown. The Bremsstrahlung in this interval will increase with a factor 4 with respect to the level measured in the wavelength interval of the twenty-channel polychromator (600-800 nm). Line radiation, however, will give a much larger contribution, especially around 400 nm where some strong O^{II} lines are located. Although the plasma volume $V_{pl} = \phi_\ell \times L \times \ell$ is much larger than in case of radial T_e -measurements, the collection efficiency $\Omega \cdot V_{pl}$ will only be a factor 1.7 more:

a. $T_{e,\perp}$ -measurement. $V_{pl} \times \Omega = 4.1 \times 10^{-8} \text{ sr} \cdot \text{m}^3$

since $\ell = 2a = 0.17 \text{ m}$

$\phi_\ell = \text{diameter of the laser beam} = 1.3 \times 10^{-3} \text{ m}$

$\Omega L = 1.96 \times 10^{-4} \text{ sr} \cdot \text{m}.$

b. $T_{e,\parallel}$ -measurement $V_{pl} \times \Omega = 6.9 \times 10^{-8} \text{ sr} \cdot \text{m}^3$

since $\ell = 0.6 \text{ m}$

$\Omega L = 8.9 \times 10^{-5} \text{ sr} \cdot \text{m}.$

The influence of the plasma-light level on the determination of the corrected signal is reduced by recording two plasma-light samples just before and after the laser pulse. A factor 2.5 improvement compared with the present situation can be achieved by reducing the ADC-integration time from 300 to 120 ns. If only Bremsstrahlung is considered, the number of recorded photo-electrons $f_{p,e}$, due to plasma light emission, as compared with those measured with the twenty-channel polychromator, can be found as follows:

- increase of the radiation 4x
- increase of collection efficiency $V_{pl} \times \Omega$: 1.7x
- increase of spectral bandwidth (from 18 nm to 75 nm) 4.2x
- reduction of the ADC-integration time 2.5x
- reduction of the observational error achieved by double plasma-light sampling $\sqrt{2}$
- experimental data from the twenty-channel polychromator:
20 photo-electrons per channel at $\lambda \approx 600$ nm and $\Delta\lambda = 18$ nm.

Hence, $f_{p,e} \approx 225$ photo-electrons generated by plasma light are expected per channel, which are to be compared with $f_{s,e} \approx 54$ from Thomson scattering.

The observational error will be:

$$\sigma = \sqrt{(f_{s,e} + f_{p,e}) + \left(\frac{f_{p,e}}{2}\right)} \quad (11)$$

and thus the relative error ϵ becomes:

$$\epsilon = \frac{\sigma}{f_{s,e}} \times 100\% = 37\% .$$

Therefore, the tail temperature and density are expected to be measured with an error of about $37\%/\sqrt{3} = 20\%$, using three of the four (see section 4) photomultipliers.

Hitherto only plasma light was considered. Stray light from the laser beam will be negligibly small because of the low stray light ratio ($10^{-5} \times T_{\text{filter}}(\lambda_0) \approx 10^{-6}$) and the low vessel stray light (which is much smaller in the tangential direction than in the radial direction).

7. CONCLUSION

Tangential Thomson scattering on TORTUR IV plasmas offers the ability to determine:

1. T_e and n_e parallel to the magnetic axis.
2. The drift velocity, v_d , from the spectral shift, $\Delta\lambda_d$, with an accuracy of 1.5×10^5 m/s at two selectable positions ($z = 0$ and 46 mm) at $n_e \approx 10^{20}$ m⁻³.
3. The current density from v_d and n_e given by:
 $j = n_e \cdot v_d \cdot e$ (A/m²).

4. The parallel tail distribution up to 20 keV at $n_e \geq 10^{18} \text{ m}^{-3}$, which is 1% of the bulk.
5. The local anomaly of the conductivity (σ) from $\sigma \propto T_e^{3/2}$ and $j = \sigma \cdot E$, assuming $E(r) = \text{constant} = V_{\text{loop}}/2\pi R$.
6. Deviations from the parallel velocity distribution, which also exist in the radial direction (satellite density $\geq 2 \times 10^{17} \text{ m}^{-3}$, 50% error).

These properties make the tangential Thomson scattering a powerful plasma diagnostic.

ACKNOWLEDGEMENT

The author wishes to thank Dr. A.J.H. Donné for his critical reading of the manuscript and H.R. Kremers who constructed the 4-channel polychromator.

This work was performed as part of the research programme of the association agreement of Euratom and the "Stichting voor Fundamenteel Onderzoek der Materie" (FOM) with financial support from the "Nederlandse Organisatie voor Zuiver-Wetenschappelijk Onderzoek" (ZWO) and Euratom.

REFERENCES

- [1] D.E. Evans and J. Katzenstein, Rep. Prog. Phys. 32 (1969) 207.
- [2] F. Alladio and M. Martone, Phys. Lett. 60A (1977) 39.
- [3] N.J. Lopes Cardozo, C.J. Barth, B. de Groot, H.A. van der Laan, H.J. van der Meiden, W. van Toledo, W.A. de Zeeuw, H. de Kluiver, Proc. 13th Eur. Conf. on Contr. Fusion and Plasma Heating, Schliersee (1986) p. 76.
- [4] C.J. Barth, "A high transmission, 20-channel polychromator for the Thomson-scattering diagnostic of TORTUR III", Rijnhuizen Report 84-156 (1984).

- [5] H. de Kluiver, N. Yousef, B. de Groot, C.J. Barth, H.J. van der Meiden, H.A. van der Laan, R.H. van Veen, F. Huussen, N.J. Lopes Cardozo, A.F.G. van der Meer, M.A.J.R. Eligh, H.E. Smulders, H.W. Piekaar, R.M. Niestadt, T. Oyevaar, Proc. 10th Int. Conf. on Plasma Phys. and Contr. Nucl. Fusion Res., Londen (1984) Vol. 1, p. 375.
- [6] R. Bartiromo, P. Buratti, L. Pieroni, O. Tudisco, IXth Eur. Conf. Oxford (1979) p. 47.
- [7] M.A. Blokh and N.F. Larionova, Sov. J. Plasma Phys. 7, (1981) p. 31.
- [8] L. Pieroni and S.E. Segre, Phys. Rev. Lett. 34 (1975) p. 928.
- [9] H. de Kluiver, N. Yousef, B. de Groot, C.J. Barth, H.A. van der Laan, N.J. Lopes Cardozo, H.J. van der Meiden, W. van Toledo, W.A. de Zeeuw, E.J. Puik, Proc. 12th Conf. on Contr. Fusion and Plasma Phys., Budapest (1985) Vol. 9F-II, p. 272.
- [10] R.M.J. Sillen, NOTEC, a code to simulate ECE spectra of plasmas which include non-thermal populations, Rijnhuizen Report 86-165 (1986).
- [11] F.B. Hendriks and H.J.B.M. Brocken, Ion temperatures in TORTUR III, Rijnhuizen Report 85-162 (1985).
- [12] R.M.J. Sillen, H.W. Piekaar, T. Oyevaar, W. Werner, Infrared Phys. 24 (1984) p. 511.
- [13] M. Mattioli and R. Papoular, Analysis of light-scattering data from relativistic plasmas, Plasma Phys. 17, (1974) 165.
- [14] H. de Kluiver, C.J. Barth and A.J.H. Donné, (submitted to Plasma Phys. & Controlled Fusion).
- [15] N.J. Lopes Cardozo, Soft X-ray electron temperature measurements on TORTUR, Rijnhuizen Report 84-151 (1984).
- [16] F. Huussen, S. Ikezawa and H. de Kluiver, Plasma Phys. & Controlled Fusion 27, (1985) 447.